EUKARYOTIC CELL, Dec. 2004, p. 1609–1618 Vol. 3, No. 6
1535-9778/04/$08.00+0 DOI: 10.1128/EC.3.6.1609–1618.2004

Snf7p, a Component of the ESCRT-III Protein Complex, Is an Upstream Member of the *RIM101* Pathway in *Candida albicans*

Amy L. Kullas, Mingchun Li, and Dana A. Davis*

Department of Microbiology, University of Minnesota, Minneapolis, Minnesota

Received 13 August 2004/Accepted 8 October 2004

The success of *Candida albicans* as an opportunistic pathogen is based in part on its ability to adapt to diverse environments. The *RIM101* pathway governs adaptation to neutral-alkaline environments and is required for virulence. Analysis of a genomic two-hybrid study conducted with *Saccharomyces cerevisiae* revealed that components involved in multivesicular bodies (MVB) transport may interact with *RIM101* pathway members. Thus, we hypothesized that these proteins may function in the *RIM101* pathway in *C. albicans*. We identified *C. albicans* homologs to *S. cerevisiae* Snf7p, Vps4p, and Bro1p and generated mutants in the cognate gene. We found that *snf7*Δ/Δ mutants, but not *vps4*Δ/Δ nor *bro1*Δ/Δ mutants, had phenotypes similar to, but more severe than, those of *RIM101* pathway mutants. We found that the constitutively active *RIM101-405* allele partially rescued *snf7*Δ/Δ mutant phenotypes. The *vps4*Δ/Δ mutant had subtle phenotypes, but these were not rescued by the *RIM101-405* allele. Further, we found that the *snf7*Δ/Δ, *vps4*Δ/Δ, and *bro1*Δ/Δ mutants did not efficiently localize the vital dye FM4-64 to the vacuole and that it was often accumulated in an MVB-like compartment. This phenotype was not rescued by *RIM101-405* or observed in *RIM101* pathway mutants. These results suggest that Snf7p may serve two functions in the cell: one as a *RIM101* pathway member and one for MVB transport to the vacuole.

All organisms must be able to respond to at least transient changes in environmental pH for survival. In fact, many organisms, such as fungi, can grow under a wide range of pH conditions. For example, *Candida albicans*, an opportunistic pathogen of humans, can grow under in vitro conditions ranging from pH 2 to 10 (7, 29). Further, *C. albicans* occurs as a commensal organism in most immunocompetent individuals and colonizes mucosal surfaces of the oral-pharyngeal, gastrointestinal, and urogenital tracts (5). These sites can show dramatic variation in extracellular pH. Thus, *C. albicans* must be able to sense and respond to changes in environmental pH to survive within the host.

The ability of fungi to sense and respond to neutral-alkaline environments is governed, at least in part, by the conserved *RIM101* pathway (referred to as the *PacC* pathway in *Aspergillus nidulans*) (7, 11). In neutral-alkaline conditions, Rim101p, the zinc finger transcription factor, promotes changes in gene expression, acting as an inducer of neutral-alkaline response genes and a repressor of acidic response genes (3, 9, 20, 34, 36). Rim101p activity is governed by proteolytic processing (14, 15, 21–23). In neutral-alkaline environments, the C-terminal D/E-rich tail of Rim101p/PacC is proteolytically cleaved to yield an active N-terminal domain, which contains the three zinc fingers. In acidic environments, Rim101p/PacC is either not proteolytically processed or processed into a form distinct from that seen at neutral-alkaline pH. Processing is governed by a number of upstream gene products, including Rim13p/PalB, which encodes a calpain-like protease; Rim20p/PalA, which interacts with the D/E-rich domain; Rim8p/PalF, which has no known function; and Rim21p/PalH and Rim9p/PalI, which encode putative transmembrane domain proteins and may serve as the environmental pH sensors (9, 12, 13, 22, 24, 27, 28, 32, 35, 42).

Despite the identification of these upstream *RIM101* pathway members, relatively little is known about how the pH signal is transmitted through this pathway to Rim101p. In fact, the only direct interaction between the known pathway members is between Rim20p and Rim101p. Xu and Mitchell demonstrated that in *S. cerevisiae*, ScRim20p interacts with the C-terminal D/E-rich domain of ScRim101p and is required for processing, leading to the hypothesis that Rim20p may promote recruitment of the likely protease Rim13p (42). Xu and Mitchell also found that *C. albicans* Rim20p interacts with CaRim101p by two-hybrid interaction. Finally, an interaction between PalA (Rim20p) and PacC (Rim101p) has also been observed with *A. nidulans* (39). Since so few interactions have been detected between the *RIM101* pathway members, it seemed probable that other components may exist that bridge the gap between the known *RIM101* pathway members.

S. cerevisiae is a powerful and elegant genetic system. It exists stably as a haploid or a diploid, can maintain plasmids, and was the first eukaryotic genome to be sequenced. Thus, *S. cerevisiae* has proved extremely amenable to the application of genomic studies. To begin to determine all the protein-protein interactions that occur within a cell, Ito et al. utilized a genomic two-hybrid strategy (18). With the results from these studies, two components of the *RIM101* pathway, Rim20p and Rim13p, were found to interact with Snf7p (Fig. 1). Further, Rim20p was also found to interact with Vps4p, a protein previously found to interact with Snf7p (37). In a separate approach, Bro1p, which has homology to Rim20p, was found to interact with Vps4p and Snf7p (16).

* Corresponding author. Mailing address: Department of Microbiology, University of Minnesota, 1360 Mayo Building MMC196, 420 Delaware St., Minneapolis, MN 55455. Phone: (612) 624-1912. Fax: (612) 626-0623. E-mail: dadavis@umn.edu.

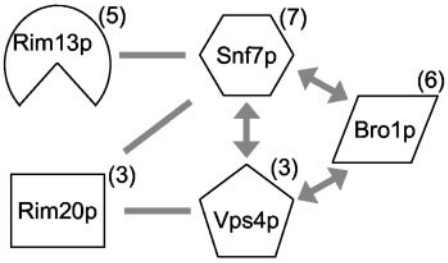

FIG. 1. A genomic two-hybrid screening identified proteins that may interact with members of the *RIM101* pathway in *S. cerevisiae* (18). These studies suggested that Snf7p and Vps4p interact with each other and with Rim20p. Further, they suggest that Snf7p also interacts with Rim13p. Vps4p can be immunoprecipitated with Snf7p and the Rim20p homolog Bro1p (16). Gray lines represent a two-hybrid interaction; gray double-sided arrows represent an interaction identified by tandem affinity purification (16). Numbers in parentheses represent the total number of two-hybrid interactions observed for a given protein.

Snf7p, Vps4p, and Bro1p function in the transport of late endosomal compartments, multivesicular bodies (MVB), to the vacuole (33). Transport of MVB to the vacuole requires three protein complexes (termed ESCRTs, for "endosomal sorting complex required for transport"). Snf7p is a cytoplasmic coiled-coil protein of the ESCRT-III protein complex that is recruited to endosomal membranes (1, 2, 19). Vps4p is a cytoplasmic AAA-type ATPase that functions in all three ESCRT protein complexes to recycle components, including Snf7p, for subsequent rounds of MVB sorting (1, 2). Bro1p is a cytoplasmic protein that associates with MVB in a Snf7p-dependent manner and also requires Vps4p for dissociation (30).

Rim20p and Rim13p are predicted to act at the same point of the *RIM101* pathway (on Rim101p itself) and may interact with ESCRT-III components of the MVB sorting machinery. Thus, we predicted that these components may be additional *RIM101* pathway members, a hypothesis previously suggested by Xu and Mitchell with respect to *S. cerevisiae* (42). In this study, we identified the *C. albicans* homologs of *S. cerevisiae* Snf7p, Vps4p, and Bro1p and demonstrated through mutant analysis that Snf7p, but not Vps4p nor Bro1p, is a member of the *RIM101* pathway. Further, we present evidence that suggests two distinct functions for Snf7p, the first as a *RIM101* pathway member and the second in MVB transport.

METHODS AND MATERIALS

Strains and plasmids. The *C. albicans* strains used in this study are derivatives of BWP17 (41) and are described in Table 1. The *snf7*Δ/Δ mutant (DAY534) was generated as follows. BWP17 was transformed with the *snf7*::*ARG4* cassette, which was amplified in a PCR using the SNF7 5DR and SNF7 3DR (Table 2) primers and the pRS-ArgΔSpe template (41), to generate the heterozygous mutant DAY530. DAY530 was then transformed with the *snf7*::*URA3-dpl200* cassette, which was amplified in a PCR using the SNF7 5DR and SNF7 3DR primers and the pDDB57 template (40), to generate the homozygous mutant DAY534. Correct integration was demonstrated by the PCR using SNF7 5detect and SNF7 3detect, which flank the site of integration (Fig. 2A).

The *vps4*Δ/Δ mutant (DAY537) were created in a similar manner. BWP17 was transformed with the *vps4*::*ARG4* cassette, which was amplified in a PCR using the VPS4 5DR and VPS4 3DR primers and the pRS-ArgΔSpe template, to generate the heterozygous mutant DAY531. This strain was then transformed with the *vps4*::*URA3-dpl200* cassette, which was amplified in a PCR using the VPS4 5DR and VPS4 3DR primers and the pDDB57 template, to generate the homozygous mutant DAY537. Correct integration was demonstrated by the PCR using VPS4 5detect and VPS4 3detect, which also flank the site of integration (Fig. 2B).

The *bro1*Δ/Δ mutant (DAY653) was generated in an analogous fashion. BWP17 was transformed with the *bro1*::*ARG4* cassette, which was amplified in a PCR using the BRO1 5DR and BRO1 3DR primers and the pRS-ArgΔSpe template, to generate the heterozygous strain DAY648. This strain was then transformed with the *bro1*::*URA3-dpl200* cassette, which was amplified in a PCR using the BRO1 5DR and BRO1 3DR primers and the pDDB57 template, to generate the homozygous mutant DAY653. Correct integration was demonstrated by the PCR using BRO1 5′detect and BRO1 3′detect, which flank the site of integration (Fig. 2C).

To complement the *snf7*Δ/Δ mutant, wild-type *SNF7* sequence was amplified in a PCR using genomic DNA from BWP17 and primers SNF7 5′comp and SNF7 3′ comp. The resulting PCR product, which contains 1,000 nucleotides upstream and 721 nucleotides downstream of the *SNF7* coding sequence, was cloned into pGEM-T Easy (Promega) to generate pDDB268. The *SNF7* sequence was removed from pDDB268 by PvuII digestion and in vivo recombined into NotI/EcoRI-digested pDDB78. pDDB267, the resulting plasmid, was recovered into DH5α *Escherichia coli* by electroporation and transformed into *C. albicans* following NruI digestion to generate DAY761. The empty vector pDDB78 was also transformed into DAY534 following NruI digestion to yield DAY763. Plasmids pDDB61 and pDDB71 (9) were digested with PpuMI to introduce the wild-type *RIM101* and constitutively active *RIM101-405* alleles into DAY534 to yield DAY544 and DAY546, respectively. To test for Rim101p processing, plasmid pDDB233 (22) was transformed into DAY534 following NruI digestion.

Media and growth conditions. *C. albicans* was routinely grown in YPD plus uridine (2% Bacto Peptone, 1% yeast extract, 2% dextrose, and 80 μg of uridine per ml). Selection for the Arg^+ and Ura^+ transformants was done on synthetic medium (0.67% yeast nitrogen base plus ammonium sulfate and without amino acids–2% dextrose–80 μg of uridine per ml was used except when selecting for *URA3* and was supplemented as required in accordance with the auxotrophic needs of the cells). M199 medium (Gibco BRL) was buffered to pH 8.0 with 150 mM HEPES and supplemented with 80 μg of uridine per ml (9).

Protein preparation and Western blot analyses. Cells were diluted 40-fold from overnight YPD plus uridine cultures into fresh M199 medium buffered with 150 mM HEPES to pH 4 or pH 7 and grown 4 h at 30°C. Cells were pelleted and stored at −80°C prior to protein extraction. Cell pellets were resuspended in ice-cold radioimmunoprecipitation assay buffer containing 1 μg of leupeptin/ml, 2 μg of aprotinin/ml, 1 μg of pepstatin/ml, 1 mM phenylmethylsulfonyl fluoride, and 10 mM dithiothreitol and transferred to glass test tubes containing acid-washed glass beads. Cells were lysed by vortexing four times for 2 min followed by 2 min on ice. Cellular debris was pelleted, and supernatants were removed and stored at −80°C. For Western blot analysis, 20 μl of 2× sodium dodecyl sulfate-polyacrylamide gel electrophoresis (SDS-PAGE) sample buffer was added to 20 μl of supernatant and samples were boiled for 5 min. Samples were loaded onto an SDS–8% PAGE gel and run overnight at 35 V. Proteins were transferred to nitrocellulose and blocked. Anti-V5 horseradish peroxidase antibody (Invitrogen) in 30 ml of 5% nonfat milk TBS-T solution (1:7,500 dilution; 50 mM Tris-HCl [pH 7.6], 150 mM NaCl, 0.05% Tween 20) was added to the blot for 4 h at 4°C. Blots were washed in TBS-T, incubated with ECL reagent (Amersham Biosciences), and exposed to film.

FM4-64 staining. YPD plus uridine cultures were grown overnight at 30°C. The following day, 25 μl of the overnight culture was added into 1 ml of M199 medium (pH 8) and then incubated for 3 to 3.5 h at 36.5°C. A total of 2.5 μl of 16 mM FM4-64 (Molecular Probes) in dimethyl sulfoxide was added to each culture, and the mixture was incubated on ice for 30 min. During this 30-min incubation, cells were examined and photographed (time = 0). Cells were then pelleted, washed with 1 ml of M199 medium (pH 8), and resuspended in 1 ml of M199 medium (pH 8). At this point, 80 μl of cells were taken and added to ice-cold tubes containing 10 μl of 100 mM sodium azide and 10 μl of 100 mM sodium fluoride (time = postincubation). The remainder of the culture was incubated at 37°C to more accurately reflect the mammalian host environment. At various time intervals, 80 μl of each sample was taken and stored on ice with 10 μl of 100 mM sodium azide and 10 μl of 100 mM sodium fluoride prior to microscopic examination and photographing.

Filamentation assays. Cultures of M199 medium (pH 8) and YPD–20% bovine calf serum were inoculated with a 1/100 dilution of an overnight YPD culture, and the cultures were incubated at 37°C for 5 and 2 h, respectively. Cells were then pelleted, washed with 1 ml of double-distilled water, and fixed in 70% ethyl alcohol for 30 min. Fixed cells were then washed and resuspended in 10 mM Tris-HCl (pH 7.4)–1 mM EDTA. Each strain was analyzed in triplicate, and at least 300 cells were counted for each sample.

TABLE 1. Strains used in this study

Strain	Background	Genotype	Reference or source
BWP17	SC5314	*ura3*::λ*imm434*/*ura3*::λ*imm434 arg4*::*hisG*/*arg4*::*hisG his1*::*hisG*/*his1*::*hisG*	41
DAY5	BWP17	*ura3*::λ*imm434*/*ura3*::λ*imm434 arg4*::*hisG*/*arg4*::*hisG his1*::*hisG*/*his1*::*hisG rim101*::*ARG4*/*rim101*::*URA3*	41
DAY23	BWP17	*ura3*::λ*imm434*/*ura3*::λ*imm434 arg4*::*hisG*/*arg4*::*hisG his1*::*hisG*/*his1*::*hisG rim20*::*ARG4*/*rim20*::*URA3*	9
DAY25	BWP17	*ura3*::λ*imm434*/*ura3*::λ*imm434 arg4*::*hisG*/*arg4*::*hisGHIS1*::*hisG*::*his1*/*his1*::*hisG rim101*::*ARG4*/*rim101*::*URA3*	8
DAY61	BWP17	*ura3*::λ*imm434*/*ura3*::λ*imm434 arg4*::*hisG*/*arg4*::*hisG his1*::*hisG*/*his1*::*hisG rim8*::*ARG4*/*rim8*::*URA3*	9
DAY185	BWP17	*ura3*::λ*imm434*/*ura3*::λ*imm434 HIS1*::*his1*::*hisG*/*his1*::*hisG ARG4*::*URA3*::*arg4*::bp*hisG*/*arg4*::*hisG*	8
DAY286	BWP17	*ura3*::λ*imm434*/*ura3*::λ*imm434 ARG4*::*URA3*::*arg4*::*hisG*/*arg4*::*hisG his1*::*hisG*/*his1*::*hisG*	10
DAY349	BWP17	*ura3*::λ*imm434*/*ura3*::λ*imm434 arg4*::*hisG*/*arg4*::*hisG his1*::*hisG*/*his1*::*hisG rim13*::*ARG4*/*rim13*::*URA3*	22
DAY530	BWP17	*ura3*::λ*imm434*/*ura3*::λ*imm434 arg4*::*hisG*/*arg4*::*hisG his1*::*hisG*/*his1*::*hisG snf7*::*ARG4*/*SNF7*	This study
DAY531	BWP17	*ura3*::λ*imm434*/*ura3*::λ*imm434 arg4*::*hisG*/*arg4*::*hisG his1*::*hisG*/*his1*::*hisG vps4*::*ARG4*/*VPS4*	This study
DAY534	DAY530	*ura3*::λ*imm434*/*ura3*::λ*imm434 arg4*::*hisG*/*arg4*::*hisG his1*::*hisG*/*his1*::*hisG snf7*::*ARG4*/*snf7*::*URA3-dpl200*	This study
DAY537	DAY531	*ura3*::λ*imm434*/*ura3*::λ*imm434 arg4*::*hisG*/*arg4*::*hisG his1*::*hisG*/*his1*::*hisG vps4*::*ARG4*/*vps4*::*URA3-dpl200*	This study
DAY544	DAY534	*ura3*::λ*imm434*/*ura3*::λ*imm434 arg4*::*hisG*/*arg4*::*hisG his1*::*hisG*/*his1*::*hisG snf7*::*ARG4*/*snf7*::*URA3-dpl200 RIM101*::*HIS1*::*RIM101*/*RIM101*	This study
DAY546	DAY534	*ura3*::λ*imm434*/*ura3*::λ*imm434 arg4*::*hisG*/*arg4*::*hisG his1*::*hisG*/*his1*::*hisG snf7*::*ARG4*/*snf7*::*URA3-dpl200 RIM101-405*::*HIS1*::*RIM101*/*RIM101*	This study
DAY568	DAY534	*ura3*::λ*imm434*/*ura3*::λ*imm434 arg4*::*hisG*/*arg4*::*hisG pHIS1*::*RIM101-V5-Age1*::*his1*::*hisG*/*his1*::*hisG snf7*::*ARG4*/*snf7*::*URA3-dpl200*	
DAY643	DAY349	*ura3*Δ::λ*imm434*/*ura3*Δ::λ*imm434 pHIS1*::*RIM101-V5-age1*::*his1*::*hisG*/*his1*::*hisG arg4*::*hisG*/*arg4*::*hisG rim13*::*URA3*/*rim13*::*ARG4*	22
DAY648	BWP17	*ura3*::λ*imm434*/*ura3*::λ*imm434 arg4*::*hisG*/*arg4*::*hisG his1*::*hisG*/*his1*::*hisG bro1*::*ARG4*/*BRO1*	This study
DAY653	DAY648	*ura3*::λ*imm434*/*ura3*::λ*imm434 arg4*::*hisG*/*arg4*::*hisG his1*::*hisG*/*his1*::*hisG bro1*::*ARG4*/*bro1*::*URA3-dpl200*	This study
DAY664	DAY537	*ura3*::λ*imm434*/*ura3*::λ*imm434 arg4*::*hisG*/*arg4*::*hisG his1*::*hisG*/*his1*::*hisG vps4*::*ARG4*/*vps4*::*URA3-dpl200 RIM101-405*:::*HIS1*::*RIM101*/*RIM101*	This study
DAY761	DAY534	*ura3*::λ*imm434*/*ura3*::λ*imm434 arg4*::*hisG*/*arg4*::*hisG HIS1*::*SNF7*::*his1*::*hisG*/*his1*::*hisG snf7*::*ARG4*/*snf7*::*URA3-dpl200*	This study
DAY763	DAY534	*ura3*::λ*imm434*/*ura3*::λ*imm434 arg4*::*hisG*/*arg4*::*hisG HIS1*::*hisG*::*his1*/*his1*::*his1*/*his1*::*hisG snf7*::*ARG4*/*snf7*::*URA3-dpl200*	This study

RESULTS

***SNF7* is required for growth at alkaline pH and on high concentrations of lithium.** We predicted that if members of the ESCRT-III complex functioned to activate Rim101p, then loss-of-function mutants in *SNF7*, *VPS4*, and *BRO1* would have phenotypes similar to other *RIM101* pathway mutants. To test this hypothesis with *C. albicans*, we utilized the TBLASTN computer algorithm (http://www-sequence.stanford.edu:8080/btcontigs6.html) to identify the *C. albicans* homologs of *S. cerevisiae SNF7*, *VPS4*, and *BRO1*. We found that orf19.6040, orf19.4339, and orf19.1670 can encode proteins 49 or 62%, 75 or 82%, and 24 or 47% identical or similar to *S. cerevisiae*

TABLE 2. Primers used in this study

Primer	Sequence
SNF7 5DR	ACTTTATTATATTAATTATAACTTTAGTTGACTGAATAAAACTTGAATAGTAAACATGTGTTTCCCAGTCACGACGTT
SNF7 3DR	TAATATATGTTTCTATACAAAGCTTTCGTTATTCTCCGTATTCGGTATTTCAAACACATCGTGGAATTGTGAGCGGATA
SNF7 5detect	AACGACAAATCAACACCAGG
SNF7 3detect	TGTGTTATCAAAAAACAGGG
VPS4 5DR	CACTATTACAAATCATATAGACTGATTTAAACTTATAAAACAATACACTTAAGCATGTCGTTTCCCAGTCACGACGTT
VPS4 3DR	TATAGAAATGAATATTTCTTGAATATATTTTATTCATTGGCCCCTCTTTTAATTACCTTCGTGGAATTGTGAGCGGATA
VPS4 5detect	GCGATTTTCAAAGATGTCGG
VPS4 3detect	AGAATTGATAGCGAAGACG
BRO1 5DR	ATGAAAACACATTTACTTGTTGTTCCAAGTAAGAAAACTGAAGAGGTTAATTGGGTCAAATTTCCCAGTCACGACGTT
BRO1 3DR	CTATTTACTGGAGAAAAAATTATACATATTTGGATTATAAGTTGAAGGATTATCATAAATGTGGAATTGTGAGCGGATA
BRO1 5′detect	TTATCCTTACATCCTTTCCG
BRO1 3′detect	TCAAGCTTTTTACCGTACGC
SNF7 5′comp	GCCTCATTGAGCAACTTGAG
SNF7 3′comp	TAATCGACATTAAAGGACTC

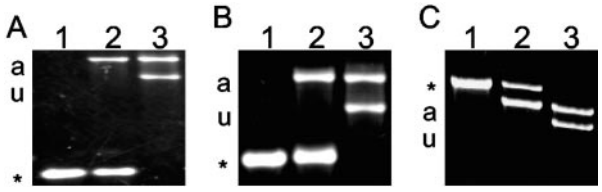

FIG. 2. Confirmation of mutants. PCR genotyping for the *snf7*Δ/Δ (A), *vps4*Δ/Δ (B), and *bro1*Δ/Δ (C) mutants was performed using primers that flank the gene of interest; the results of representative PCR analysis of genomic DNA from the wild type (lanes 1; BWP17 in each case), a heterozygous mutant (lanes 2; DAY530, DAY531, and DAY648, respectively), and a homozygous mutant (lanes 3; DAY534, DAY537, and DAY653, respectively) are shown. The wild-type (*), *ARG4* allele (a), and *URA3* allele (u) bands are noted to the left of each sample.

Snf7p, Vps4p, and Bro1p, respectively. To determine whether these genes encode members of the *RIM101* pathway, we generated insertion-deletion mutants by PCR product-directed gene disruption (41). Homologous integrants were identified via PCR with primers that flank the integration site (Fig. 2). We were able to recover independent homozygous mutants with all three genes, which suggests that these genes are not essential for growth.

The *RIM101* pathway is required for growth on alkaline medium and in the presence of high concentrations of lithium. Thus, we first analyzed the *snf7*Δ/Δ, *vps4*Δ/Δ, and *bro1*Δ/Δ mutants for growth on these media. On rich medium, the heterozygous mutants and the *rim101*Δ/Δ, *rim20*Δ/Δ, *vps4*Δ/Δ, and *bro1*Δ/Δ homozygous mutants grew at rates similar to those seen with the wild type (Fig. 3B and 4). However, the *snf7*Δ/Δ homozygous mutant appeared to have slightly reduced growth (Fig. 3B and 4A; compare the growth results for individual colonies in the most dilute lanes). Identical results were observed for independent *snf7*Δ/Δ, *vps4*Δ/Δ, and *bro1*Δ/Δ mutants (data not shown). On rich medium buffered to pH 9 or containing 150 mM lithium chloride, the growth seen with the heterozygous mutants and the *vps4*Δ/Δ and *bro1*Δ/Δ homozygous mutants was similar to wild-type growth results. However, the *rim101*Δ/Δ, *rim20*Δ/Δ, and *snf7*Δ/Δ mutants showed a severe reduction in growth on these media (Fig. 3C and D and 4A). In fact, the *snf7*Δ/Δ mutant showed a more severe growth defect than either the *rim101*Δ/Δ or the *rim20*Δ/Δ mutant. These results suggest that *VPS4* and *BRO1* do not have a significant role in growth at alkaline pH or in the presence of

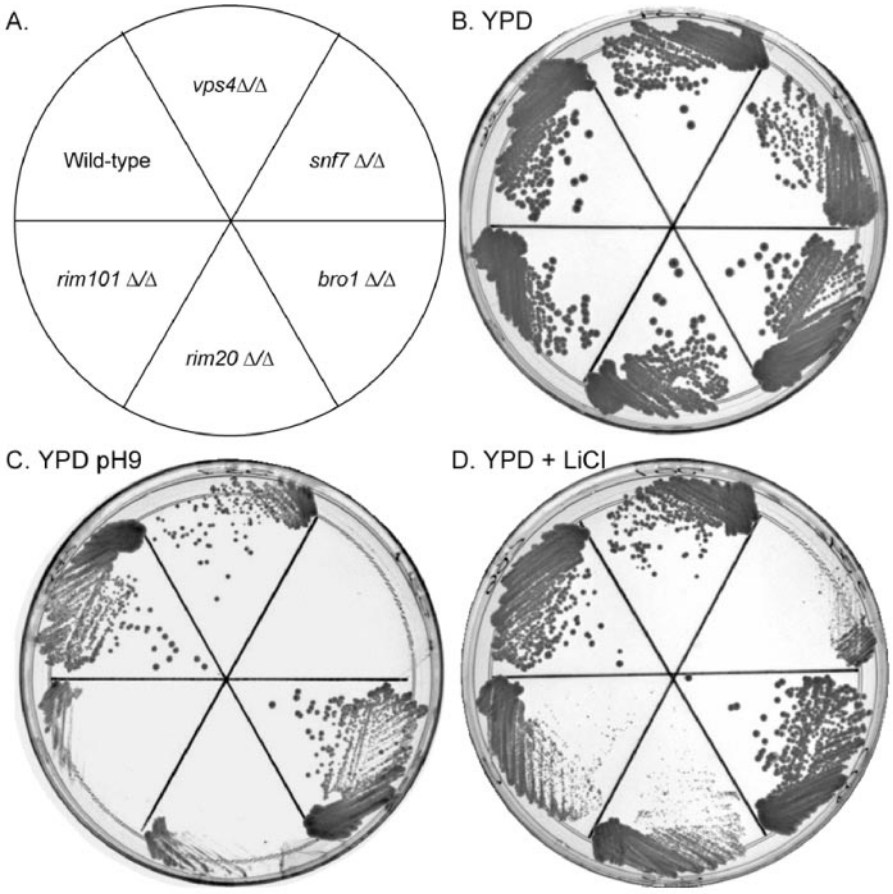

FIG. 3. Growth phenotypes of ESCRT-III mutants. (A) The locations of the strains analyzed were as follows: wild-type (DAY286), *vps4*Δ/Δ (DAY537), *snf7*Δ/Δ (DAY534), *bro1*Δ/Δ (DAY653), *rim20*Δ/Δ (DAY23), and *rim101*Δ/Δ (DAY5). (B to D) Strains were grown on YPD (B), YPD (pH 9) (C), and YPD plus LiCl (D) for 2 days at 37°C prior to photographing.

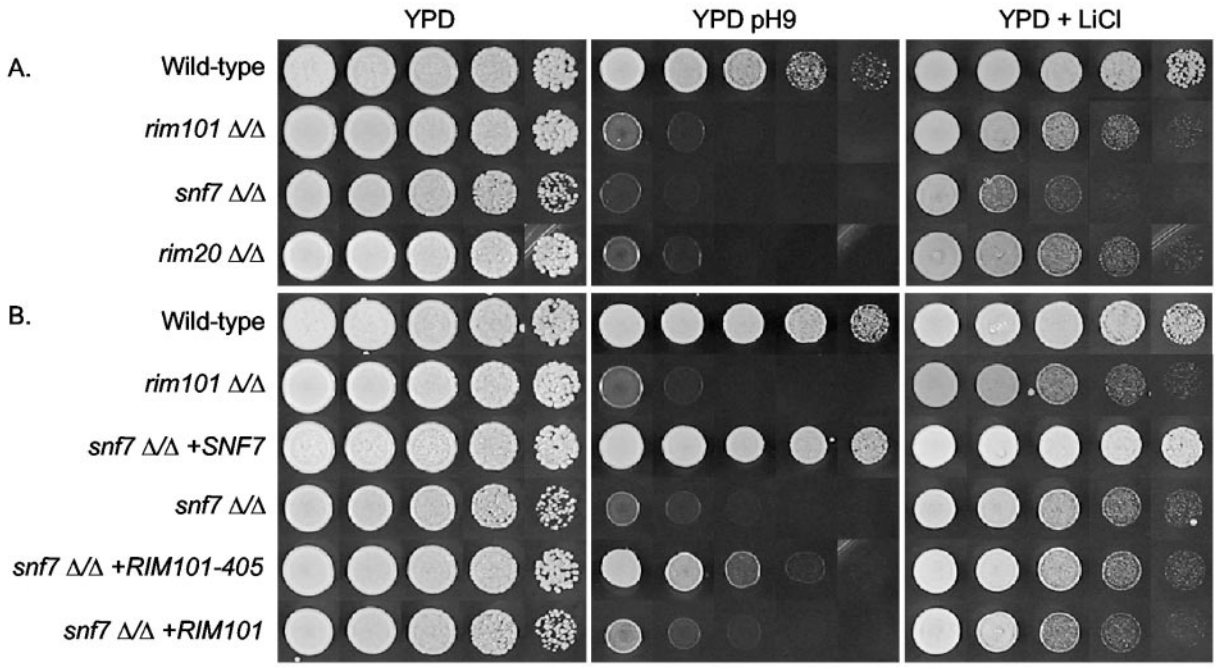

FIG. 4. Growth phenotypes by spot dilutions. (A) His$^-$ wild-type (DAY286), *rim101*Δ/Δ (DAY5), *snf7*Δ/Δ (DAY534), and *rim20*Δ/Δ (DAY23) strains were serially diluted fivefold and plated on YPD, YPD at pH 9, and YPD plus LiCl and grown at 37°C. (B) Prototrophic wild-type (DAY185), *rim101*Δ/Δ (DAY25), *snf7*Δ/Δ *SNF7* (DAY761), *snf7*Δ/Δ (DAY763), *snf7*Δ/Δ *RIM101-405* (DAY546), and *snf7*Δ/Δ *RIM101* (DAY544) strains were serially diluted fivefold and plated on YPD, YPD at pH 9, and YPD plus LiCl and grown at 37°C. Plates were grown for 24 h prior to photographing.

high concentrations of lithium. These results also suggest that *SNF7* has a critical role for growth on these media.

We considered the possibility that the alkaline pH and lithium growth phenotypes of the *snf7*Δ/Δ mutant were not due to loss of *SNF7* sequence or to a specific defect in the *RIM101* pathway. To test these possibilities, we first reintroduced a wild-type copy of *SNF7* into the *snf7*Δ/Δ mutant. Introduction of wild-type *SNF7* rescued the slow growth defect on rich medium and restored growth on pH 9 and 150 mM LiCl medium to levels indistinguishable from that seen with the wild type (Fig. 4B). Introduction of the empty vector into the *snf7*Δ/Δ mutant did not rescue these phenotypes to wild-type levels; however, we noted that these prototrophic *snf7*Δ/Δ strains did appear to grow better on pH 9 medium and LiCl medium than the His$^-$ auxotrophic strains (Compare Fig. 4A and B). These results demonstrate that the growth phenotypes observed with the *snf7*Δ/Δ mutant are due to the loss of *SNF7* sequence.

Next, we introduced the constitutively active *RIM101-405* allele into the *snf7*Δ/Δ mutant, which bypasses the requirement for the upstream members of the *RIM101* pathway (9). If the *snf7*Δ/Δ growth phenotypes are due to defects in the *RIM101* pathway, then the *RIM101-405* allele should rescue the *snf7*Δ/Δ mutant. Indeed, expression of *RIM101-405* in the *snf7*Δ/Δ background rescued the slight growth defect on YPD medium and partially restored growth on pH 9 medium (Fig. 4), but expression of an additional wild-type copy of *RIM101* in the *snf7*Δ/Δ background did not. However, *RIM101-405* did not significantly improve *snf7*Δ/Δ growth on LiCl medium. These results suggest that the alkaline growth phenotypes of the *snf7*Δ/Δ mutant can be partially rescued by the constitutively active *RIM101-405* allele, providing support for the hypothesis that *SNF7* encodes an upstream member of the *RIM101* pathway. Further, these results indicate that Snf7p has additional functions independent of the *RIM101* pathway.

***SNF7* is required for filamentation.** The *RIM101* pathway positively regulates filamentation on a variety of media (9, 22, 32, 34). Thus, we asked whether *SNF7*, *VPS4*, and *BRO1* are required for filamentation. On solid M199 medium (pH 8), the wild type, the heterozygous mutants, and the *bro1*Δ/Δ homozygous mutant formed yeast colonies with extensive peripheral filaments (Fig. 5A and data not shown). The *vps4*Δ/Δ homozygous mutant also formed yeast colonies with peripheral filaments; however, filamentation was not as robust as that seen with wild-type cells. Finally, the *snf7*Δ/Δ homozygous mutant formed yeast colonies that lacked peripheral filaments on M199 medium (pH 8) similar to those seen with the *rim101*Δ/Δ and the *rim20*Δ/Δ mutants (Fig. 5). As observed for the growth phenotypes described above, we found that introduction of a wild-type copy of *SNF7* into the *snf7*Δ/Δ mutant completely rescued the filamentation defect but that the empty vector did not. Further, introduction of the *RIM101-405* allele into the *snf7*Δ/Δ mutant partially restored filamentation, but an additional wild-type copy did not. Introduction of the *RIM101-405* allele into the *vps4*Δ/Δ mutant did not rescue the partial filamentation defect (Fig. 5), suggesting that this phenotype is unrelated to the *RIM101* pathway. Similar results were observed in liquid M199 medium (pH 8). These results support the hypothesis that Snf7p encodes an upstream member of the

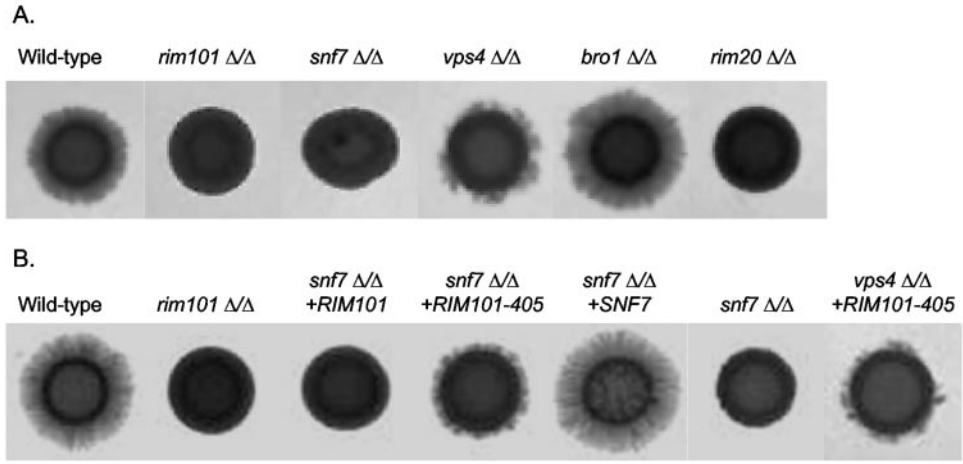

FIG. 5. Alkaline-induced filamentation of ESCRT-III mutants. (A) Wild-type (DAY286), *rim101*Δ/Δ (DAY5), *snf7*Δ/Δ (DAY534), *vps4*Δ/Δ (DAY537), *bro1*Δ/Δ (DAY653), and *rim20*Δ/Δ (DAY23) strains were grown overnight in YPD and spotted onto M199 medium (pH 8). (B) Complementation studies of the *snf7*Δ/Δ mutant. Wild-type (DAY185), *rim101*Δ/Δ (DAY25), *snf7*Δ/Δ *RIM101* (DAY544), *snf7*Δ/Δ *RIM101-405* (DAY546), *snf7*Δ/Δ *SNF7* (DAY761), and *snf7*Δ/Δ (DAY763) strains were grown overnight in YPD and spotted onto M199 medium (pH 8). Plates were incubated at 37°C for 5 days prior to photographing.

RIM101 pathway and has functions independent of the *RIM101* pathway.

We next analyzed filamentation in serum. In liquid serum, wild-type, *vps4*Δ/Δ, and *bro1*Δ/Δ cells formed germ tubes and grew in the filamentous form (Table 3). As described previously, the *rim101*Δ/Δ mutant showed a ~16% reduction in germ tube formation and filamentous growth compared to the wild type ($P < 0.002$) (22). The *snf7*Δ/Δ mutant had a more severe defect in germ tube formation, a ~49% reduction compared to the wild type ($P < 1 \times 10^{-5}$), and a ~39% reduction compared to the *rim101*Δ/Δ mutant ($P < 3 \times 10^{-4}$). Introduction of the *RIM101-405* allele rescued the *snf7*Δ/Δ mutant compared to the results seen with an additional wild-type copy of *RIM101* ($P < 5 \times 10^{-5}$). However, in similarity to the results described above, *RIM101-405* only partially rescued the *snf7*Δ/Δ mutant, leading to a filamentation level similar to that seen with the *rim101*Δ/Δ mutant ($P < 0.09$) but not similar to that seen with wild-type cells. These results support the idea that Snf7p has Rim101p-dependent and -independent functions.

***SNF7* is required for Rim101p processing.** Rim101p is activated by proteolytic processing, which is governed by the upstream members of the *RIM101* pathway. Thus, if Snf7p is an upstream member of the *RIM101* pathway, then Rim101p processing should be altered in a *snf7*Δ/Δ mutant. To address this possibility, we introduced a V5-epitope-tagged version of Rim101p, Rim101-V5p (22), into the *snf7*Δ/Δ mutant and analyzed Rim101p processing by Western blotting.

In wild-type cells at pH 4, Rim101-V5p was found in two forms of 85 and 65 kDa (Fig. 6). In wild-type cells at pH 7, Rim101-V5p was found primarily in two forms of 85 and 74 kDa; however, the 65-kDa form could also be observed. As reported previously, the *rim13*Δ/Δ mutant lacked the 74- and 65-kDa forms and only the 85-kDa form was observed (Fig. 6) (22). With the *snf7*Δ/Δ mutant, only the 85-kDa form of Rim101-V5p was observed at pH 4 and pH 7, in similarity to the results seen with the *rim13*Δ/Δ mutant. These results demonstrate that Snf7p is required for both Rim101p processing events in *C. albicans* and support the model that Snf7p is an upstream member of the *RIM101* pathway.

***SNF7*, *VPS4*, and *BRO1* are required for endocytosis.** In *S. cerevisiae*, *SNF7*, *VPS4*, and *BRO1* encode proteins that function in MVB transport to the vacuole (33). To determine whether the *SNF7*, *VPS4*, and *BRO1* gene products identified in *C. albicans* carry out a similar function, we analyzed endocytic transport from the plasma membrane to the vacuole by use of the fluorescent marker FM4-64 (38). In wild-type cells, FM4-64 was initially seen at the plasma membrane (Fig. 7). However, FM4-64 was rapidly internalized into endocytic vesicles and was localized to the vacuolar membrane within 45 min. After 90 min, essentially only vacuolar membrane staining remained. In *snf7*Δ/Δ, *vps4*Δ/Δ, and *bro1*Δ/Δ mutant cells, FM4-64 was initially seen at the plasma membrane and was rapidly found within endocytic vesicles. However, unlike wild-type cell results, FM4-64 was delayed in progression to the vacuole. After 45 min, vacuolar membrane staining was not apparent, although the vacuole was often surrounded by diffuse staining. After 90 min, the vacuole could be visualized in the *vps4*Δ/Δ and *bro1*Δ/Δ mutants, although cytoplasmic stain-

TABLE 3. Filamentation in liquid serum medium

Strain	Relevant genotype	% of filamentation in serum[a]
DAY286	Wild type	88.3
DAY5	*rim101*Δ/Δ	74.1[b]
DAY534	*snf7*Δ/Δ	45.3[b,c]
DAY544	*snf7*Δ/Δ *RIM101*	44.4[b,c]
DAY546	*snf7*Δ/Δ *RIM101-405*	78.9[b]
DAY537	*vps4*Δ/Δ	84.7
DAY653	*bro1*Δ/Δ	93.7

[a] Results represent the average of three independent experiments. Standard deviation <5%.
[b] Statistically different from the wild-type result by analysis of variance.
[c] Statistically worse than the *rim101*Δ/Δ mutant result by analysis of variance.

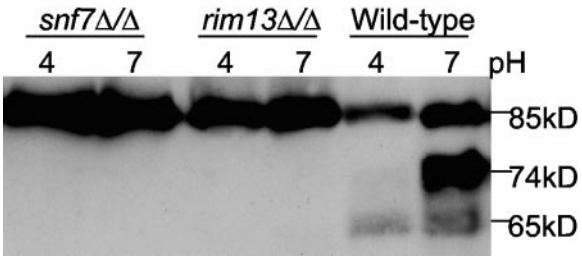

FIG. 6. Western blot analysis for Rim101p processing. Wild-type (DAY492), *rim13*Δ/Δ (DAY643), and *snf7*Δ/Δ (DAY568) strains that express Rim101-V5p were grown 4 h at pH 4 and 7. Protein was purified and separated by SDS–8% PAGE. Gels were transferred to nitrocellulose and probed with anti-V5 horseradish peroxidase (Invitrogen).

ing by endocytic vesicles remained. However, the *snf7*Δ/Δ mutant still had poorly stained vacuolar membranes and primarily revealed diffuse staining. After 150 min, these three mutants still maintained diffuse staining in the cytoplasm, although the *snf7*Δ/Δ mutant was clearly the most defective. Although vacuolar staining could be observed in the *vps4*Δ/Δ, *bro1*Δ/Δ, and (to a lesser extent) *snf7*Δ/Δ mutants, we often observed brighter staining caps of FM4-64 on one side of the vacuole (Fig. 7). This phenomenon has also been described for *S. cerevisiae* and likely reflects FM4-64 localization to a late endocytic-prevacuolar (MVB-like) compartment (30, 38). Thus, these results suggest that Snf7p, Vps4p, and Bro1p play a role in MVB transport to the vacuole and that Snf7p has a critical role in this process.

Since *SNF7* appears to function in the *RIM101* pathway, we asked whether the *RIM101* pathway functions in the MVB transport. To address this possibility, we first asked whether the *RIM101-405* allele rescues the *snf7*Δ/Δ endocytic defect. While introduction of the *RIM101-405* allele into the *snf7*Δ/Δ mutant partially rescued the growth and filamentation defects of the *snf7*Δ/Δ mutant, FM4-64 localization to the vacuole was not significantly improved (Fig. 8A). However, introduction of a wild-type copy of *SNF7* into the *snf7*Δ/Δ mutant completely restored the FM4-64 localization to the vacuole. Thus, the function of Snf7p for MVB transport to the vacuole does not require activated Rim101p.

Finally, we tested whether other *RIM101* pathway members were required for FM4-64 localization. Unlike the Snf7p, Vps4p, and Bro1p results, the four previously described

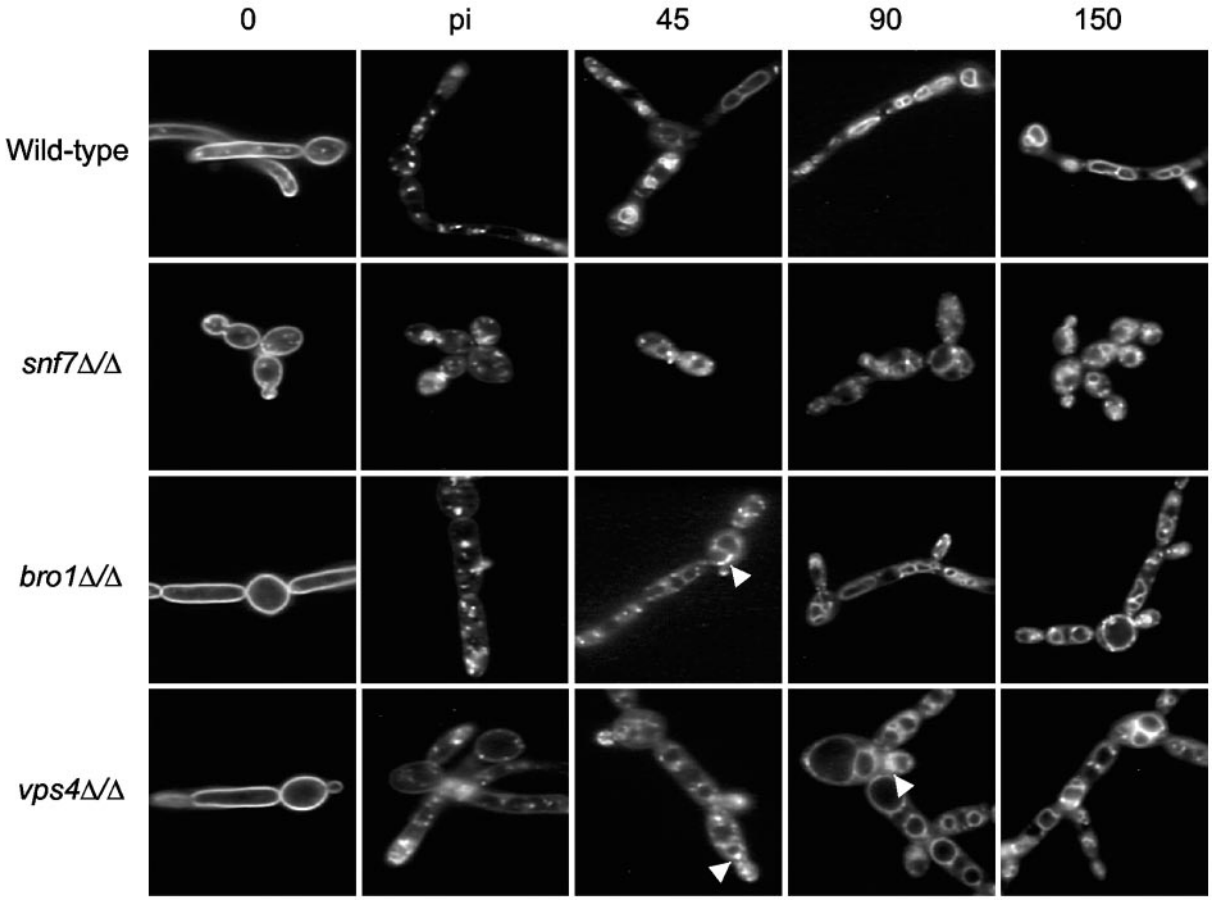

FIG. 7. FM4-64 staining in ESCRT-III mutants. Wild-type (DAY286), *snf7*Δ/Δ (DAY534), *vps4*Δ/Δ (DAY537), and *bro1*Δ/Δ (DAY653) strains were incubated 30 min on ice in M199 medium (pH 8) containing 16 mM FM4-64 (time = 0). Cells were then pelleted, washed, and resuspended in warm M199 medium (pH 8) lacking FM4-64 (time = postincubation). Cells were incubated at 37°C, and at 45-, 90-, and 150-min intervals aliquots were taken and transferred to ice-cold tubes containing sodium azide and sodium fluoride. Photographs are representative of three independent samples. pi, postincubation.

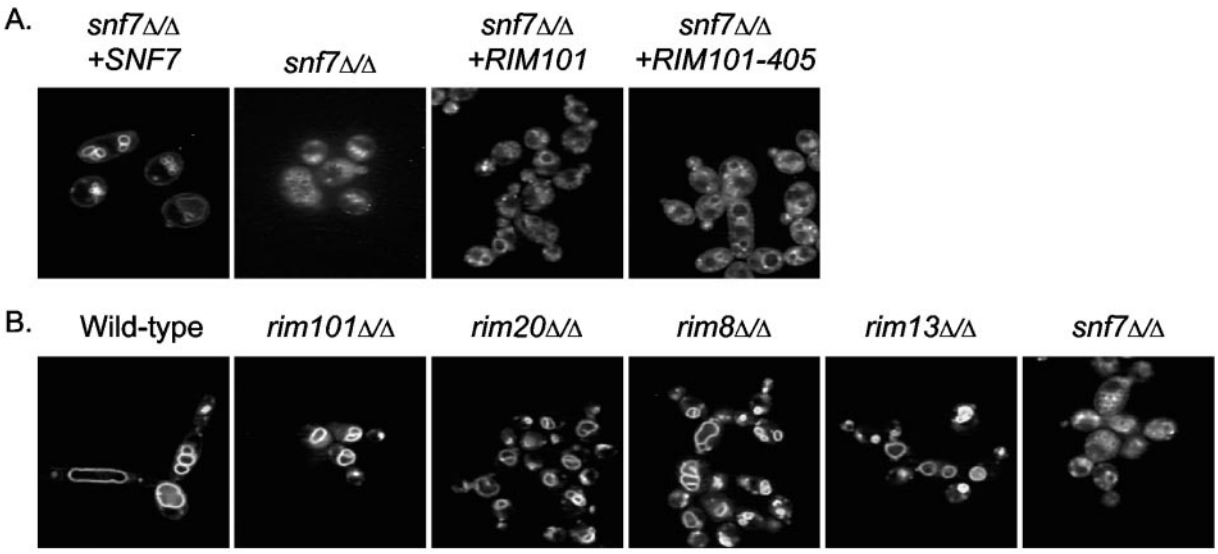

FIG. 8. FM4-64 staining complemented *snf7*Δ/Δ strains and *RIM101* pathway mutants. (A) Rescue of *snf7*Δ/Δ mutants for FM4-64 staining: *snf7*Δ/Δ *SNF7* (DAY761), *snf7*Δ/Δ (DAY763), *snf7*Δ/Δ *RIM101* (DAY544), and *SNF7*Δ/Δ *RIM101-405* (DAY546) strains were stained with FM4-64 as described for Fig. 7. Pictures represent samples taken after 60 min. (B) *RIM101* pathway mutants and FM4-64 staining: wild-type (DAY286), *rim101*Δ/Δ (DAY5), *rim20*Δ/Δ (DAY23), *rim8*Δ/Δ (DAY61), *rim13*Δ/Δ (DAY349), and *snf7*Δ/Δ (DAY534) strains were stained with FM4-64 as described for Fig. 7. Pictures represent samples taken after 120 min.

RIM101 pathway members, Rim101p, Rim8p, Rim13p, and Rim20p, were dispensable for FM4-64 localization to the vacuole (Fig. 8B). Thus, the previously identified *RIM101* pathway members are not required for MVB transport to the vacuole.

DISCUSSION

The ability of *C. albicans* to respond appropriately to changes in environmental pH is required for pathogenesis (7). This ability is governed in part by the *RIM101* pathway at neutral-alkaline pH. Here, we have identified Snf7p, an ESCRT-III component, as a new member of the *RIM101* pathway in *C. albicans*. This finding is supported by several lines of evidence. First, the *snf7*Δ/Δ mutant has growth defects in environments that require the *RIM101* pathway, including alkaline pH and high lithium concentrations. Second, the *snf7*Δ/Δ mutant has filamentation defects under conditions of stimuli that require the *RIM101* pathway. Third, growth and filamentation defects associated with the *snf7*Δ/Δ mutant are partially restored by expression of the constitutively active *RIM101-405* allele. However, Vps4p and Bro1p, two additional ESCRT-III components, do not function in the *RIM101* pathway. Loss of Vps4p did result in a slight defect in filamentation; however, unlike the results seen with the *snf7*Δ/Δ mutant, the *RIM101-405* allele did not rescue this phenotype in the *vps4*Δ/Δ mutant. Further, we have found that Rim101p processing is absolutely dependent on Snf7p but not Vps4p (unpublished data). Further, during the revision process for the work described here, a related study also demonstrated a link between MVB transport and the *RIM101* pathway in *S. cerevisiae* and *C. albicans* (43). Thus, in total these results strongly suggest that Snf7p is an upstream member of the *RIM101* pathway.

As described for *S. cerevisiae* and higher eukaryotes, we found that Snf7p, Vps4p, and Bro1p are required for MVB for vacuole transport in *C. albicans*. However, this function is independent of the *RIM101* pathway. Again, this idea is supported by several lines of evidence. First, *snf7*Δ/Δ, *vps4*Δ/Δ, and *bro1*Δ/Δ mutant cells all fail or have a significant delay in FM4-64 localization to the vacuole compared to wild-type cells. Further, these mutants appear to accumulate MVB-like structures within the cell. Second, the previously identified *RIM101* pathway members are dispensable for vacuolar localization of FM4-64 and do not accumulate MVB-like structures. Finally, the constitutively active *RIM101-405* allele does not rescue vacuole FM4-64 localization in the *snf7*Δ/Δ mutant.

On the basis of these results, we propose that in *C. albicans*, Snf7p functions in the *RIM101* pathway and as an ESCRT-III component and that these two functions are distinct (Fig. 9). Since Snf7p functions in both the *RIM101* pathway and the MVB pathway, additive defects result in severe phenotypes. Further, this model predicts that constitutive activation of Rim101p would only partially rescue *snf7*Δ/Δ phenotypes, which is what we observed (Fig. 4 and 5). Analysis of the

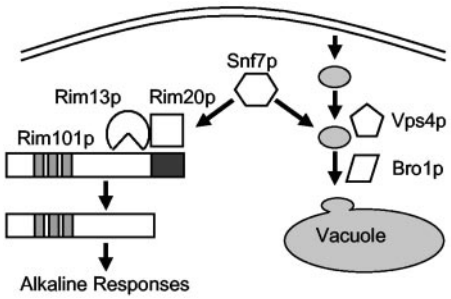

FIG. 9. Model of Snf7p function. Snf7p has two distinct functions in *C. albicans*. One function is to transport MVB to the vacuole during endocytosis. The second function is as a member of the *RIM101* pathway, which is activated in response to neutral-alkaline environments.

*vps4*Δ/Δ mutant suggests that MVB transport may be required for filamentation (Fig. 5). In fact, other studies have suggested that correct vesicle trafficking to the vacuole is required for filamentation (4, 31). However, the *bro1*Δ/Δ mutant did not have any significant defects in filamentation or growth. Bro1p appears to act very late in MVB transport, and it has been suggested that Bro1p acts downstream of the ESCRT-III complex (30). Thus, it is also possible that Bro1p acts downstream of the requirement for MVB transport for filamentation.

Why does Snf7p function link MVB transport and Rim101p activation? In alkaline environments, the plasma membrane H^+-ATPase is inhibited to prevent disruption of the proton gradient and cells utilize Ena1p, the Na^+-ATPase, to establish a sodium gradient. In both *C. albicans* and *S. cerevisiae*, *ENA1* expression is positively regulated by Rim101p (3, 20, 21). However, cells also require the vacuolar H^+-ATPase to maintain acidification of the vacuole, which in alkaline environments will be continually neutralized through the process of endocytosis (26). Genomic studies of *S. cerevisiae* have revealed that components of the endocytic machinery, including Snf7p and Vps4p, are required for wild-type rates of growth in alkaline environments, suggesting that MVB transport to the vacuole is critical under these stress conditions (17). Thus, when yeast cells encounter alkaline environments, the process of MVB transport to the vacuole is important for growth and the *RIM101* pathway is activated. Therefore, it is possible that it is a switch to dependence on the endocytic pathway for growth that activates the *RIM101* pathway.

In an *S. cerevisiae* two-hybrid screening, Vps4p was found to interact with Rim20p (18). However, our results suggest that Vps4p is not involved in the *RIM101* pathway. Bro1p, a homolog of Rim20p, can be immunoprecipitated with Vps4p (Fig. 1) and requires Vps4p to dissociate from MVB (30). Thus, there appears to be a functional link between Bro1p and Vps4p. Judging on the basis of these observations, it seems likely that the two-hybrid interaction Vps4p has with Rim20p is at a region of homology with Bro1p. In fact, studies of *S. cerevisiae* suggest that Rim20p and Bro1p have distinct functions in activation of the *RIM101* pathway and MVB transport (30, 42). Thus, while Vps4p clearly interacts with Bro1p, there does not appear to be an interaction between Vps4p and Rim20p in vivo.

The interaction between the *RIM101*/*PacC* pathway and MVB transport appears to be conserved through several distantly related ascomycetes, including *C. albicans*, *S. cerevisiae*, and *A. nidulans*. We have shown that the *RIM101* pathway is required for virulence in a systemic model of infection, and we have identified Snf7p as a new member of this pathway (7). Our results also suggest that Snf7p and Vps4p have Rim101p-independent functions in filamentation. Since the ability to switch between yeast and filamentous forms is a virulence trait (6, 25), it seems likely that the process of MVB transport to the vacuole and endocytosis as a whole may also be required for virulence. Thus, the MVB transport machinery and/or endocytosis may serve as a potential new target for antifungal therapeutics, which may work on diverse fungal pathogens.

ACKNOWLEDGMENTS

We thank Aaron P. Mitchell and Paul T. Magee for helpful discussions on this work and Samuel Martin for critical review of the manuscript. We also thank Catie Hill for help constructing the *SNF7* complementation vector. We are grateful to members of the numerous groups in the *Candida* community involved in establishing an accessible genome database and in particular to Andre Nantel and Malcolm Whiteway at the NRC Biotechnology Research Institute.

This research of Dana A. Davis was supported in part by the Investigators in Pathogenesis of Infectious Disease Award from the Burroughs Wellcome Fund.

REFERENCES

1. **Babst, M., D. J. Katzmann, E. J. Estepa-Sabal, T. Meerloo, and S. D. Emr.** 2002. Escrt-III: an endosome-associated heterooligomeric protein complex required for mvb sorting. Dev. Cell **3:**271–282.
2. **Babst, M., B. Wendland, E. J. Estepa, and S. D. Emr.** 1998. The Vps4p AAA ATPase regulates membrane association of a Vps protein complex required for normal endosome function. EMBO J. **17:**2982–2993.
3. **Bensen, E. S., S. J. Martin, M. Li, J. Berman, and D. A. Davis.** Transcriptional profiling in *C. albicans* reveals new adaptive responses to extracellular pH and functions for Rim101p. Mol. Microbiol., in press.
4. **Bruckmann, A., W. Kunkel, K. Augsten, R. Wetzker, and R. Eck.** 2001. The deletion of CaVPS34 in the human pathogenic yeast *Candida albicans* causes defects in vesicle-mediated protein sorting and nuclear segregation. Yeast **18:**343–353.
5. **Calderone, R. A.** 2002. *Candida* and candidiasis. ASM Press, Washington, D.C.
6. **Calderone, R. A., and W. A. Fonzi.** 2001. Virulence factors of *Candida albicans*. Trends Microbiol. **9:**327–335.
7. **Davis, D.** 2003. Adaptation to environmental pH in *Candida albicans* and its relation to pathogenesis. Curr. Genet. **44:**1–7.
8. **Davis, D., J. E. Edwards, Jr., A. P. Mitchell, and A. S. Ibrahim.** 2000. *Candida albicans RIM101* pH response pathway is required for host-pathogen interactions. Infect. Immun. **68:**5953–5959.
9. **Davis, D., R. B. Wilson, and A. P. Mitchell.** 2000. *RIM101*-dependent and -independent pathways govern pH responses in *Candida albicans*. Mol. Cell. Biol. **20:**971–978.
10. **Davis, D. A., V. M. Bruno, L. Loza, S. G. Filler, and A. P. Mitchell.** 2002. *Candida albicans* Mds3p, a conserved regulator of pH responses and virulence identified through insertional mutagenesis. Genetics **162:**1573–1581.
11. **Denison, S. H.** 2000. pH regulation of gene expression in fungi. Fungal Genet. Biol. **29:**61–71.
12. **Denison, S. H., S. Negrete-Urtasun, J. M. Mingot, J. Tilburn, W. A. Mayer, A. Goel, E. A. Espeso, M. A. Penalva, and H. N. Arst, Jr.** 1998. Putative membrane components of signal transduction pathways for ambient pH regulation in *Aspergillus* and meiosis in *Saccharomyces* are homologous. Mol. Microbiol. **30:**259–264.
13. **Denison, S. H., M. Orejas, and H. N. Arst, Jr.** 1995. Signaling of ambient pH in *Aspergillus* involves a cysteine protease. J. Biol. Chem. **270:**28519–28522.
14. **Diez, E., J. Alvaro, E. A. Espeso, L. Rainbow, T. Suarez, J. Tilburn, H. N. Arst, Jr., and M. A. Penalva.** 2002. Activation of the *Aspergillus* PacC zinc finger transcription factor requires two proteolytic steps. EMBO J. **21:**1350–1359.
15. **Futai, E., T. Maeda, H. Sorimachi, K. Kitamoto, S. Ishiura, and K. Suzuki.** 1999. The protease activity of a calpain-like cysteine protease in *Saccharomyces cerevisiae* is required for alkaline adaptation and sporulation. Mol. Gen. Genet. **260:**559–568.
16. **Gavin, A. C., M. Bosche, R. Krause, P. Grandi, M. Marzioch, A. Bauer, J. Schultz, J. M. Rick, A. M. Michon, C. M. Cruciat, M. Remor, C. Hofert, M. Schelder, M. Brajenovic, H. Ruffner, A. Merino, K. Klein, M. Hudak, D. Dickson, T. Rudi, V. Gnau, A. Bauch, S. Bastuck, B. Huhse, C. Leutwein, M. A. Heurtier, R. R. Copley, A. Edelmann, E. Querfurth, V. Rybin, G. Drewes, M. Raida, T. Bouwmeester, P. Bork, B. Seraphin, B. Kuster, G. Neubauer, and G. Superti-Furga.** 2002. Functional organization of the yeast proteome by systematic analysis of protein complexes. Nature **415:**141–147.
17. **Giaever, G., A. M. Chu, L. Ni, C. Connelly, L. Riles, S. Veronneau, S. Dow, A. Lucau-Danila, K. Anderson, B. Andre, A. P. Arkin, A. Astromoff, M. El-Bakkoury, R. Bangham, R. Benito, S. Brachat, S. Campanaro, M. Curtiss, K. Davis, A. Deutschbauer, K. D. Entian, P. Flaherty, F. Foury, D. J. Garfinkel, M. Gerstein, D. Gotte, U. Guldener, J. H. Hegemann, S. Hempel, Z. Herman, D. F. Jaramillo, D. E. Kelly, S. L. Kelly, P. Kotter, D. LaBonte, D. C. Lamb, N. Lan, H. Liang, H. Liao, L. Liu, C. Luo, M. Lussier, R. Mao, P. Menard, S. L. Ooi, J. L. Revuelta, C. J. Roberts, M. Rose, P. Ross-Macdonald, B. Scherens, G. Schimmack, B. Shafer, D. D. Shoemaker, S. Sookhai-Mahadeo, R. K. Storms, J. N. Strathern, G. Valle, M. Voet, G. Volckaert, C. Y. Wang, T. R. Ward, J. Wilhelmy, E. A. Winzeler, Y. Yang, G. Yen, E. Youngman, K. Yu, H. Bussey, J. D. Boeke, M. Snyder, P. Philippsen, R. W. Davis, and M. Johnston.** 2002. Functional profiling of the *Saccharomyces cerevisiae* genome. Nature **418:**387–391.
18. **Ito, T., T. Chiba, R. Ozawa, M. Yoshida, M. Hattori, and Y. Sakaki.** 2001. A comprehensive two-hybrid analysis to explore the yeast protein interactome. Proc. Natl. Acad. Sci. USA **98:**4569–4574.
19. **Kranz, A., A. Kinner, and R. Kolling.** 2001. A family of small coiled-coil-

forming proteins functioning at the late endosome in yeast. Mol. Biol. Cell **12:**711–723.
20. **Lamb, T. M., and A. P. Mitchell.** 2003. The transcription factor Rim101p governs ion tolerance and cell differentiation by direct repression of the regulatory genes *NRG1* and *SMP1* in *Saccharomyces cerevisiae*. Mol. Cell. Biol. **23:**677–686.
21. **Lamb, T. M., W. Xu, A. Diamond, and A. P. Mitchell.** 2001. Alkaline response genes of *Saccharomyces cerevisiae* and their relationship to the *RIM101* pathway. J. Biol. Chem. **276:**1850–1856.
22. **Li, M., S. J. Martin, V. M. Bruno, A. P. Mitchell, and D. A. Davis.** 2004. *Candida albicans* Rim13p, a protease required for Rim101p processing at acidic and alkaline pHs. Eukaryot. Cell **3:**741–751.
23. **Li, W., and A. P. Mitchell.** 1997. Proteolytic activation of Rim1p, a positive regulator of yeast sporulation and invasive growth. Genetics **145:**63–73.
24. **Maccheroni, W., Jr., G. S. May, N. M. Martinez-Rossi, and A. Rossi.** 1997. The sequence of *palF*, an environmental pH response gene in *Aspergillus nidulans*. Gene **194:**163–167.
25. **Mitchell, A. P.** 1998. Dimorphism and virulence in *Candida albicans*. Curr. Opin. Microbiol. **1:**687–692.
26. **Munn, A. L., and H. Riezman.** 1994. Endocytosis is required for the growth of vacuolar H(+)-ATPase-defective yeast: identification of six new *END* genes. J. Cell Biol. **127:**373–386.
27. **Negrete-Urtasun, S., S. H. Denison, and H. N. Arst, Jr.** 1997. Characterization of the pH signal transduction pathway gene *palA* of *Aspergillus nidulans* and identification of possible homologs. J. Bacteriol. **179:**1832–1835.
28. **Negrete-Urtasun, S., W. Reiter, E. Diez, S. H. Denison, J. Tilburn, E. A. Espeso, M. A. Penalva, and H. N. Arst, Jr.** 1999. Ambient pH signal transduction in *Aspergillus*: completion of gene characterization. Mol. Microbiol. **33:**994–1003.
29. **Odds, F. C.** 1988. *Candida* and candidosis, 2nd ed. Bailiere Tindall, London, England.
30. **Odorizzi, G., D. J. Katzmann, M. Babst, A. Audhya, and S. D. Emr.** 2003. Bro1 is an endosome-associated protein that functions in the MVB pathway in *Saccharomyces cerevisiae*. J. Cell Sci. **116:**1893–1903.
31. **Palmer, G. E., A. Cashmore, and J. Sturtevant.** 2003. *Candida albicans* VPS11 is required for vacuole biogenesis and germ tube formation. Eukaryot. Cell **2:**411–421.
32. **Porta, A., A. M. Ramon, and W. A. Fonzi.** 1999. *PRR1*, a homolog of *Aspergillus nidulans palF*, controls pH-dependent gene expression and filamentation in *Candida albicans*. J. Bacteriol. **181:**7516–7523.
33. **Raiborg, C., T. E. Rusten, and H. Stenmark.** 2003. Protein sorting into multivesicular endosomes. Curr. Opin. Cell Biol. **15:**446–455.
34. **Ramon, A. M., A. Porta, and W. A. Fonzi.** 1999. Effect of environmental pH on morphological development of *Candida albicans* is mediated via the PacC-related transcription factor encoded by *PRR2*. J. Bacteriol. **181:**7524–7530.
35. **Su, S. S., and A. P. Mitchell.** 1993. Identification of functionally related genes that stimulate early meiotic gene expression in yeast. Genetics **133:**67–77.
36. **Tilburn, J., S. Sarkar, D. A. Widdick, E. A. Espeso, M. Orejas, J. Mungroo, M. A. Penalva, and H. N. Arst, Jr.** 1995. The *Aspergillus* PacC zinc finger transcription factor mediates regulation of both acid- and alkaline-expressed genes by ambient pH. EMBO J. **14:**779–790.
37. **Uetz, P., L. Giot, G. Cagney, T. A. Mansfield, R. S. Judson, J. R. Knight, D. Lockshon, V. Narayan, M. Srinivasan, P. Pochart, A. Qureshi-Emili, Y. Li, B. Godwin, D. Conover, T. Kalbfleisch, G. Vijayadamodar, M. Yang, M. Johnston, S. Fields, and J. M. Rothberg.** 2000. A comprehensive analysis of protein-protein interactions in *Saccharomyces cerevisiae*. Nature **403:**623–627.
38. **Vida, T. A., and S. D. Emr.** 1995. A new vital stain for visualizing vacuolar membrane dynamics and endocytosis in yeast. J. Cell Biol. **128:**779–792.
39. **Vincent, O., L. Rainbow, J. Tilburn, H. N. Arst, Jr., and M. A. Penalva.** 2003. YPXL/I is a protein interaction motif recognized by *Aspergillus* PalA and its human homologue, AIP1/Alix. Mol. Cell. Biol. **23:**1647–1655.
40. **Wilson, R. B., D. Davis, B. M. Enloe, and A. P. Mitchell.** 2000. A recyclable *Candida albicans URA3* cassette for PCR product-directed gene disruptions. Yeast **16:**65–70.
41. **Wilson, R. B., D. Davis, and A. P. Mitchell.** 1999. Rapid hypothesis testing in *Candida albicans* through gene disruption with short homology regions. J. Bacteriol. **181:**1868–1874.
42. **Xu, W., and A. P. Mitchell.** 2001. Yeast PalA/AIP1/Alix homolog Rim20p associates with a PEST-like region and is required for its proteolytic cleavage. J. Bacteriol. **183:**6917–6923.
43. **Xu, W., F. J. Smith, Jr., R. Subaran, and A. P. Mitchell.** 2004. Multivesicular body-ESCRT components function in pH response regulation in *Saccharomyces cerevisiae* and *Candida albicans*. Mol. Biol. Cell, in press.